FEM Modelling of Tool Wear in Hard Turning Operations

To cite this article: Cristian Cappellini and Franco Concli 2021 *IOP Conf. Ser.: Mater. Sci. Eng.* **1190** 012023

FEM Modelling of Tool Wear in Hard Turning Operations

Cristian Cappellini [1], Franco Concli [1]

[1] Free University of Bolzano, Piazza Università 1, 39100 Bolzano, Italy

cristian.cappellini@unibz.it

Abstract. Hard turning is a machining operation of finishing performed on material with a hardness higher than 45 HRC and it has been demonstrated to be a profitable alternative to grinding process allowing, respect to this latter, better surface quality, improved process control reliability, and faster production rates. The high pressure and sliding velocity at the tool-chip interface, in addition to the deformation energy generated, lead to the formation of high temperature zones localized in the cutting region. These thermal loads enhance harmful aspects on both cutting tool and machined material. On the tool, the abrasive-diffusive wear mechanism is promoted. On the workpiece, a local surface heat treatment of quenching is observed, upgrading the formation of a thin layer of over-quenched martensite, called white layer, due to its appearance under microscopical observation, that is undesirable due to its brittleness and related cracks generation. In addition to this, hard turning is usually performed in dry condition further augmenting machining temperature and tool wear rate. Because of the extremely high hardness of the machined materials, the employment of expensive ultra-high hardness cutting tools is mandatory. Thus, to make the process valuable, it is essential to optimize the tool usage by avoiding catastrophic failure and being able to forecast the tool wear evolution during cutting time as a function of the applied process parameters. One of the possible approaches for predicting the wear behaviour is finite element (FE) simulations of the turning process. In this work, the wear of polycrystalline cubic boron nitride (PCBN) tools when turning AISI 52100 hardened steel is investigated. An abrasive-diffusive wear model has been developed and implemented in a FE engine, by means of a dedicated subroutine able to update the geometry of the worn tool as a function of the cutting parameters, with the intent of simulating the tool wear behaviour, in terms of crater and flank wear extension. For the calibration of the model, the tool wear measurements achieved from an experimental campaign of orthogonal cutting tests have been used. The influence of process parameters on the wear rate has been examined, underlining that the most affecting parameter on tool wear is the cutting speed: the higher the cutting speed the higher the tool wear. Furthermore, it has been observed that the tool breakage was due to an excessive depth of the crater wear that modified the initial negative rake angle to a positive one. This modification changed the stress state of the tool from compressive to tensile, not well tolerated by PCBN tools, bringing to catastrophic failure. The tool wear simulation results are in good agreement with the experimental ones, validating the usability of the proposed computational methodology for crater and flank wear prediction. Therefore, the application of this technique allows the optimization of cutting parameters from a preventive FE simulation analysis avoiding the need of exploiting new costly and time-consuming experimental tests.

1. Introduction

Hard turning is a machining process that deal with the cutting of materials whose hardness is higher than 45 HRC [1]. Compared with traditional grinding process, this technique allows a better surface

finish, an improved dimensional accuracy, and a production time reduction [2]. Hence, in the last years, hard turning has been developed as a valuable alternative to grinding [3]. Due to its widespread in the industrial filed, a good knowledge of the effects of the technological aspects, such as process parameters, physical and chemical properties of materials, and tool wear, on the final product quality is mandatory. With this intent, several studies have been accomplished, leading to the development of empirical and analytical models for the optimization of cutting parameters [4], or for the assessment of tool life [5] and tool wear [6]. This latter affects geometrical accuracy, roughness, residual stresses, and surface modifications, that are related to the localized formation of white and dark layers [7-9], thus the possibility to forecast tool wear represents a profitable way to reduce production costs [10]. Because of the hardness of the worked material, hard turning is performed with extremely hard materials, and among these, polycrystalline cubic boron nitride (PCBN) is one the most employed. The wear mechanisms of PCBN tools are mainly related to abrasion, adhesion, and diffusion [6]. Their occurrence is a function of tool chemical composition [11], namely the ratio between binder and hard particles contents (CBN), and cutting parameters [12], such as cutting speed, feed rate, and depth of cut. Aimed to predict the evolution of PCBN tool wear, analytical models [13] and artificial neural networks (ANNs) [14] have been utilized in the past, while poor are the contributions to finite element method (FEM) modeling that demonstrated to be a good methodology to characterize the tool wear behavior during the cutting time [15]. In the present work, a FEM strategy for simulating the wear of PCBN tools in hard turning of AISI 52100 steel is presented. An abrasive-diffusive tool wear model, concerning the wear on the tool rake face, defined as crater wear (*KT*), and on the tool flank (*VB*), has been developed. This model evaluates the wear rate as a function of influencing parameters, namely sliding velocity, contact temperature, and interface pressure, at the chip-tool contact interface. Its implementation in the FEM software has been achieved by the generation of a dedicated subroutine able to move the nodes of the tool mesh for updating the geometry of the worn tool. For the collection of the tool wear measurements, an extensive experimental campaign has been performed by means of several hard turning tests. The proposed methodology has been calibrated and validated by the comparison of simulated results with the experimental ones. The outcomes show good agreement between experiments and simulations, underlining the suitability of the proposed methodology for forecasting tool wear growth.

2. Materials and methods

In order to obtain the tool wear measurements, subsequently used for the calibration of the developed wear model, an experimental campaign consisting of orthogonal turning tests has been performed by the variation of the process parameters, namely cutting speed (V_C) and feed rate (f). Their values are shown in figure 1, where it can be observed that two levels have been assigned to both cutting speed and feed rate, and the relative test name. During the tests, workpiece and tool material, dry condition, depth of cut, and geometries, have been kept constant.

2.1. Workpiece preparation

The workpieces consisted of disks made of AISI 52100 hardened steel with a thickness of 1.2 mm, also representing the depth of cut, and an initial diameter of 150 mm. The selection of AISI 52100 steel material was due to its industrial relevance and hardenability. Its chemical composition, expressed in percentage in weight, is reported in table 1.

Table 1. AISI 52100 chemical composition.

Element	Fe	C	Cr	Mn	P	Si	S
% in weight	97.0	0.98-1.10	1.45	0.35	<0.025	0.230	<0.025

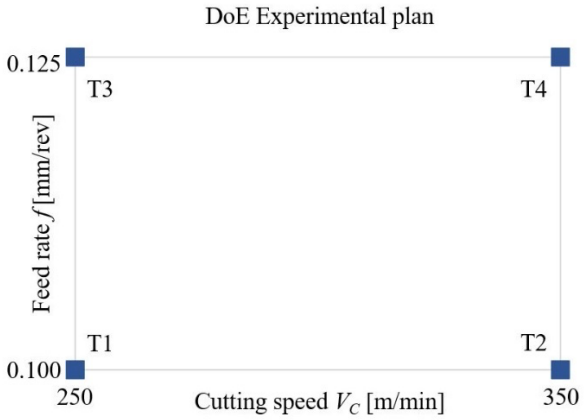

Figure 1. Values of the process parameters implemented in the experimental tests.

The specimens have been prepared by means of the heat treatment cycle of quenching and tempering described in figure 2. The application of the heat treatment was necessary in order to obtain values of mechanical properties and hardness comparable with the ones detected in common industrial applications, as reported by the standard UNI EN ISO 683-17:2014 for technical characteristics of furniture of ball bearing steels. The thermal cycle contemplates a normalization at 550 °C followed by a quenching treatment with an austenitization temperature of 860 °C. Both normalization and quenching are performed in a salt furnace. This technique is mandatory to allow a uniform heating of the disk and to prevent excessive deformation since, the low thickness increases the thermal distortion effect. For the same reason, a salt bath maintained at 175 °C is used as quenching medium. After quenching, the cooling at environment temperature, is completed in air, giving a hardness that ranges between 63 HRC and 65 HRC. To achieve the desired hardness, the specimen is then tempered in furnace at 390 °C. At the end of the tempering treatment, the disk is left to cool in air, leading to the desired hardness of 57 HRC. Finally, the disks are gently ground to obtain a flat surface of the requested thickness.

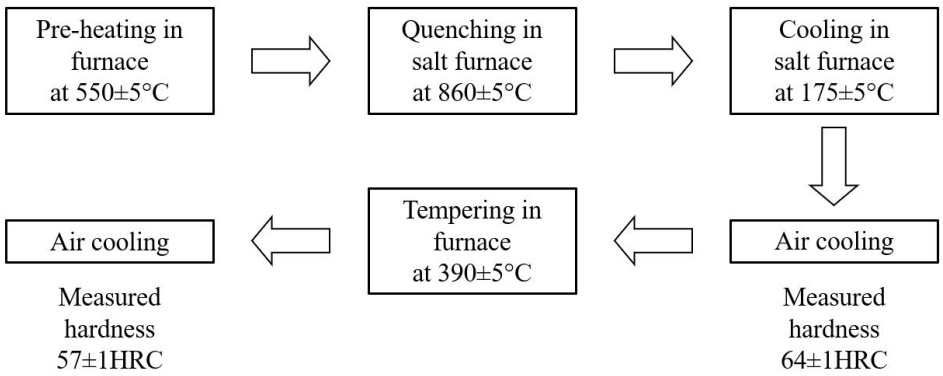

Figure 2. Heat treatment cycle of the specimens.

2.2. Cutting tests and tool wear measurements

The orthogonal cutting tests has been carried out in dry condition on a computer numerical control (CNC) lathe furnishing a nominal power of 7 kW. The tool employed was a PCBN insert ISO TNGN 110308S-01020 CBN100 by Seco Tools, where cubic-boron-nitride particles are dispersed in a TiC binder matrix. The properties of the insert are reported in table 2. To provide a negative rake angle (γ) of -8°, an inclination angle (λ) of 0°, and an entering angle (χ) of 90°, a toolholder

ISO CTFNR3225P11-PL was adopted. A specifically designed equipment, visible in figure 3, was used to fix the disks on the mandrel.

Table 2. PCBN tool properties.

CBN content	Binder	Hardness	Young's modulus	Poisson's ratio	Thermal expansion	Thermal conductivity
50%	TiC	27.5 HK	588 GPa	0.153	6.2 10^{-6} 1/K	40 W/mK

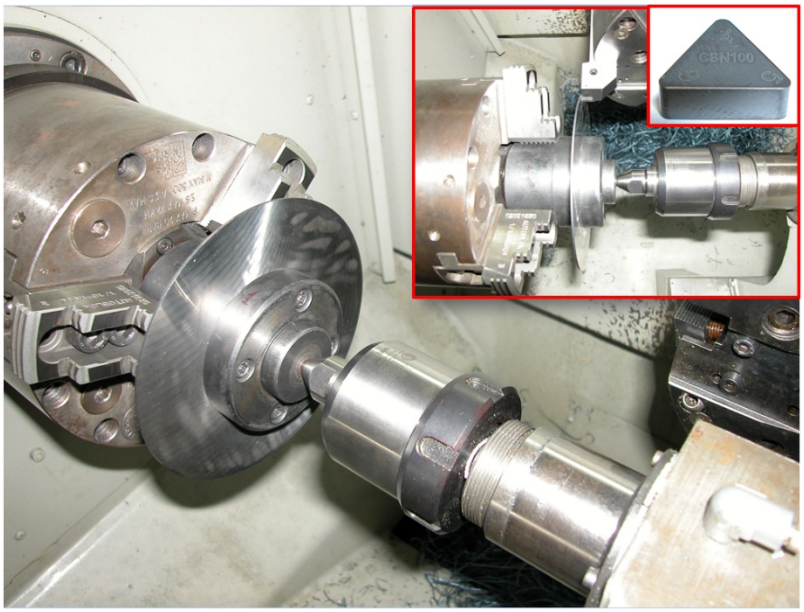

Figure 3. Experimental setup for orthogonal cutting tests.

As indicated by the tool-life testing standard ISO 3685:1993, throughout each test the flank wear (*VB*), and crater wear (*KT*) have been measured at regular time intervals. The catastrophic tool breakage has been chosen as the end of each tool-life test. In order to determine the time intervals for each test, the estimation of the final tool life is needed. For the evaluation of the tool life, an analytical model developed in [5] has been employed. This model correlates the process parameters with the tool life and is reported in equation (1):

$$V_C \cdot T_L^G \cdot f^E \cdot d_C^F \cdot \left(\frac{H}{H_0}\right)^D = C \quad (1)$$

where V_C is the cutting speed in [m/min], T_L is the tool-life in [min], f is the feed rate in [mm/rev], d_C is the depth of cut in [mm], H is the workpiece hardness in [HRC], H_0 is a reference hardness equal to 60 HRC, C is a constant equal to 172, G, E, F, and D, are exponents calibrated as a function of workpiece and tool material, respectively equal to 0.285, 0.335, 0.112, and 1.07. The tool life values calculated by equation (1) were found in accordance with the experimental ones. The cutting time intervals have been calculated dividing the total tool life approximately in 10 sub-steps except for the tests concerning a cutting speed of 350 m/min, where a lower number of sub-steps were used. For detecting the flank wear at each sub-step, the insert was removed from the toolholder and measured by means of an optical coordinate measuring machine CMM (Mitutoyo QS200) with a resolution of 0.5 μm and an accuracy lower than 2.5 μm. A typical flank wear measurement is visible in figure 4a. Crater wear depth was acquired by means of a profilometer (Mitutoyo SJ-301) with a resolution of 0.01 μm. Concerning the measurement of the crater wear depth, several profiles on the worn tool rake

face have been acquired at regular spatial intervals of 0.1 mm, as shown in figure 4b, and among these the maximum value of *KT* has been selected as the representative crater wear depth.

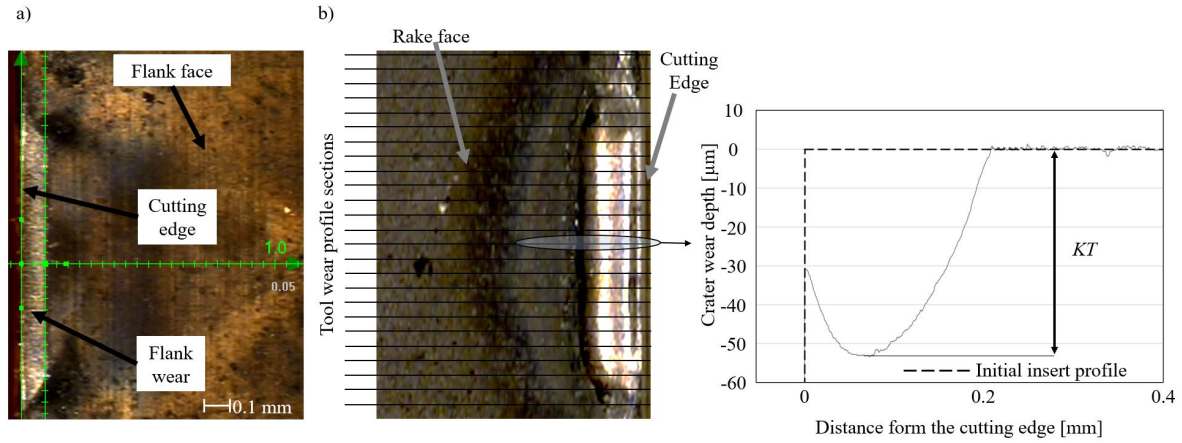

Figure 4. a) Flank wear measurement technique, and b) crater wear measurement technique (test T1, cutting time = 150s).

2.3. The developed tool wear model

The development of a coupled abrasive-diffusive tool wear model is determined to consider the different wear mechanisms acting on rake and flank face of the insert. In particular, the part of the model concerning crater wear is a combination of abrasion and diffusion contribution, while, due to the high hardness of worked material, the flank wear is modelled by pure abrasion, as observed in [12]. Because of the low CBN content of the employed tool, the adhesive contribution in the proposed model is neglected [6]. This assumption has been also confirmed by the observation of the worn tool (figure 5), where no adherent workpiece material is visible.

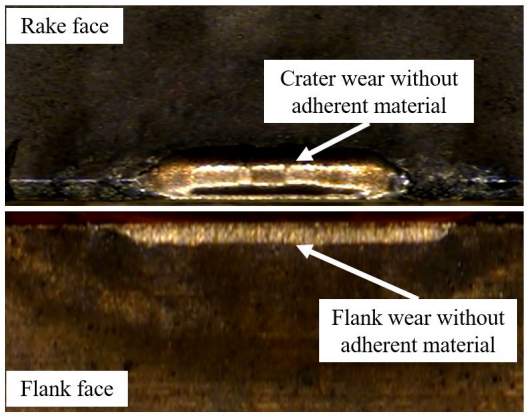

Figure 5. Rake and flank face of the tool without adherent material (test T3, cutting time = 130s).

Equation (2) reports the expression for the implemented tool wear model; Where $\partial W_{KT}/\partial t$ and $\partial W_{VB}/\partial t$ are the tool wear rate for rake and flank face respectively, H_{wp} [N/mm2] and H_t [N/mm2] are temperature hardness functions for workpiece and tool respectively, $K_Q = 20460$ is a constant related to the activation energy for diffusion, v_S [mm/s] is the sliding velocity at tool-chip interface, σ_n [MPa] is the contact pressure at tool-chip interface, T_{int} [°C] is the temperature at tool-chip interface, V_C [mm/s] is the cutting speed, $K = 0.416$ and $n = 7.0$ are hardness constant and hardness exponent whose values are dependent from the workpiece-tool hardness ratio. The coefficients $K_{KT\_abr} = 0.735$, $K_{KT\_diff} = 24602$, and $K_{VB\_abr} = 0.085$ that are respectively related to the abrasive crater wear, the

diffusive crater wear, and the abrasive flank wear, have been calibrated by comparing the worn tool geometry simulation results with the experimental measurements of crater and flank wear of the first cutting sub-step for all the tests. The simulation software provides the values of contact pressure (σ_n), sliding velocity (v_S), and interface temperature (T_{int}) in their local values. For the flank wear model, the sliding velocity is assumed equal to the cutting speed (V_C). The tool wear model calculates the value of wear rate for each mesh node of the tool and subsequently, the implemented subroutine moves the tool nodes, to update the worn tool geometry.

$$\begin{cases} \frac{\partial W_{KT}}{\partial t} = K_{KT_{abr}} \cdot K \cdot \left(\frac{H_{wp}^{n-1}}{H_t^n}\right) \cdot v_S \cdot \sigma_n + K_{KT_{diff}} \cdot \sqrt{v_S} \cdot e^{-K_Q/(T_{int}+273)} & for\ crater\ wear \\ \frac{\partial W_{VB}}{\partial t} = K_{VB_{abr}} \cdot K \cdot \left(\frac{H_{wp}^{n-1}}{H_t^n}\right) \cdot V_C \cdot \sigma_n & for\ flank\ wear \end{cases} \quad (2)$$

$$H_{wp} = 11760 \cdot exp(-16.3 \cdot 10^{-4} T_{int})$$

$$H_t = 45000 - 4.324 T_{int}$$

2.4. FEM simulations

The cutting experiments have been faithfully reproduced, in terms of cutting parameters, materials, lubrication condition, in the FE environment. Figure 6 shows the FEM model with tool and workpiece at the beginning (figure 6a) and during the simulation (figure 6b) where the chip formation is evident.

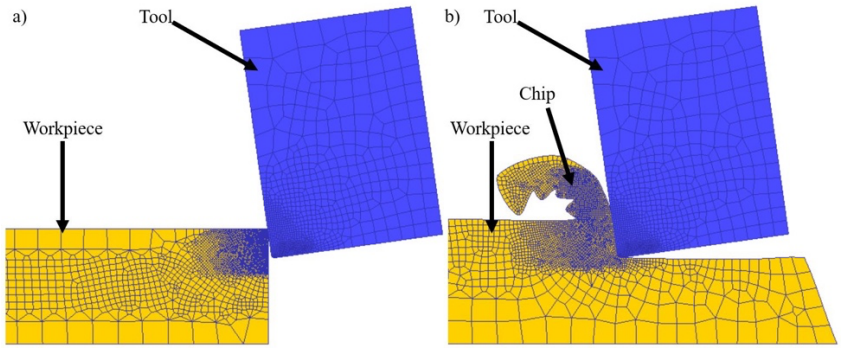

Figure 6. FEM model, a) initial simulation step, b) chip formation during simulation.

The workpiece has been considered as a rigid-plastic object and discretized with a mesh of more than 5000 quadrilateral linear elements. The rigid-plastic behavior of the workpiece material has been characterized by the modified Johnson-Cook's model of equation (3) proposed in [16], where ε is the strain, ε_r is the strain rate, T is the local temperature, $B(T)$ is a polynomial function of temperature, $J(HRC)$ and $I(HRC)$ are functions of the hardness, while $A = 0.0567$, $L = 1092$ MPa, $p = 0.083$, $m = 0.1259$, $M = 0.3$, $r = 5$, and $S = 20$ are constants.

$$\sigma = B(T)[L\varepsilon^p + J(HRC) + I(HRC)\varepsilon][1 + (ln(\varepsilon_r^m) - A)]\left[M + (1 + M)\left[tanh\left(\frac{1}{\varepsilon^r}\right)\right]^S\right] \quad (3)$$

The tool has been modelled as a rigid object and meshed with more than 1000 quadrilateral linear elements. A finer mesh, in the correspondence of the tool-chip contact area, has been created, achieving a minimum element size of 3 μm for both the objects, and allowing a correct evaluation of generated and exchanged heat between them. The initial temperature of both tool and workpiece has been set equal to 20 °C. The heat transfer coefficient (*htc*) of the two objects with the environment, applied on their free surfaces, has been set equal to 20 W/m^{2}K, while at the tool-chip interface *htc* has been imposed equal to 45000 W/m^{2}K. In order to represent the dry cutting conditions, the Zorev's hybrid frictional model [17] has been implemented. This model subdivides the tool-chip contact area in two zones: a sticking zone from the tool edge up to two times the feed, where the frictional stresses

are equal to the shear flow stress of the workpiece, and a sliding zone in the remaining contact length where the frictional stresses are proportional to the contact pressure. In the proposed model the proportionality constant was set equal to 0.35.

To correctly simulate T_{int}, σ_n, and v_S at the tool-chip interface, it is mandatory to reach the thermo-mechanical steady-state before the application of the tool wear subroutine. With this intent, the simulation strategy reported in figure 7 has been adopted. In the first stage of the procedure an incremental Lagrangian (IL) solver is applied to reach the mechanical steady-state. The subsequent thermal steady-state is then achieved by the exploitation of an arbitrary Lagrangian-Eulerian (ALE) solver. After this, the subroutine for tool wear rate calculation and the geometry update of the worn tool is called. Here, the tool wear rate is calculated for each tool node in accordance with the rake or flank tool wear model of equation (2). Based on the time interval and estimated wear rate, the tool wear is determined, and the tool geometry is updated. The update of the geometry is performed by the movement of the nodes of a quantity equal to the estimated wear in the opposite direction respect the outgoing normal of the elements at which the nodes are connected. Once the tool geometry is updated, the IL solver is employed again to reach a new thermo-mechanical steady-state considering the worn tool topology. The described technique is iteratively applied until the total machining time is reached. An example of simulated tool wear evolution is visible in figure 8.

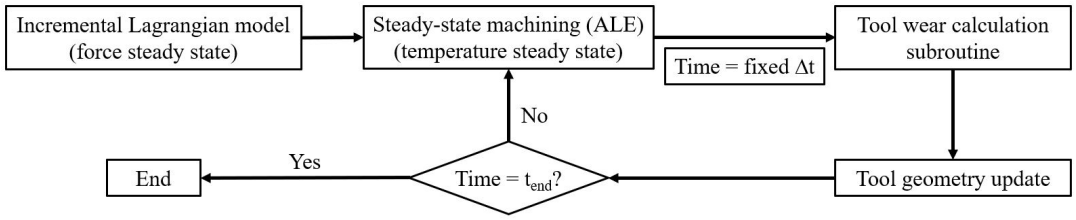

Figure 7. Applied simulation strategy.

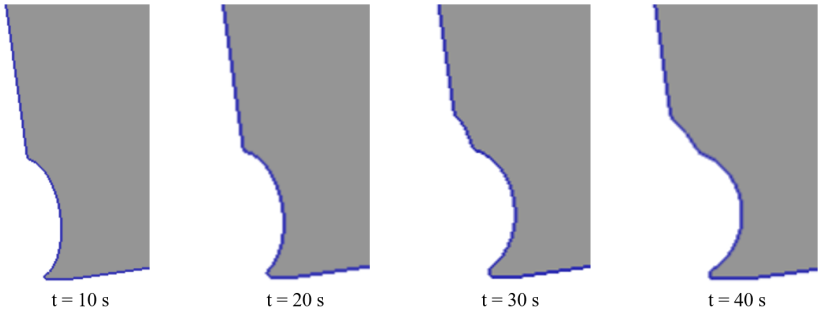

Figure 8. Example of simulated tool wear evolution (test T2).

3. Results and discussion

3.1. Experimental results

In figure 9 the evolutions of flank (*VB*) and crater (*KT*) wear during the cutting time of each test are visible. It is evident that both flank (figure 9a) and crater (figure 9b) wear are deeply influenced by the cutting speed: the higher the cutting speed the higher the tool wear rate. Moreover, the feed rate does not reveal considerable effects of the flank wear rate. In contrast, the influence of feed rate on the crater wear evolution is more prominent especially at lower cutting speed. This behavior is due to the diffusive wear mechanism that is higher with the raise of temperature. An increased feed rate leads to a higher chip section area that requires greater cutting forces. At constant cutting speeds, this means that more power is required for the machining operation, thus the deformation energy augments too. The deformation energy in the chip is converted in heat that increases the cutting temperature and

consequently the diffusion mechanism is enhanced. The analysis of *KT* evolution indicates that the insert breakage occurs when the crater depth is slightly higher than 60 μm. The severe crater wear on the PCBN inserts leads to a modification of the tool rake angle from an initial negative value to a positive one (figure 10a). This geometric alteration reduces the resistant section area of the tool and increases the tensile stresses at which the resistant section is subjected. The low strength of PCBN tools to tensile stresses, brings to the premature failure of the insert. This behavior has been also verified by a simulation of the mechanical stresses on the tool during the cutting (figure 10b).

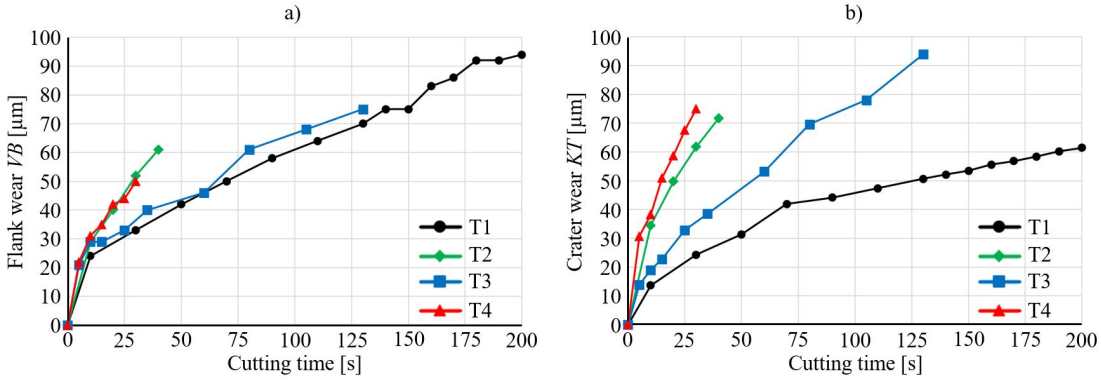

Figure 9. Example of simulated tool wear evolution (test T2).

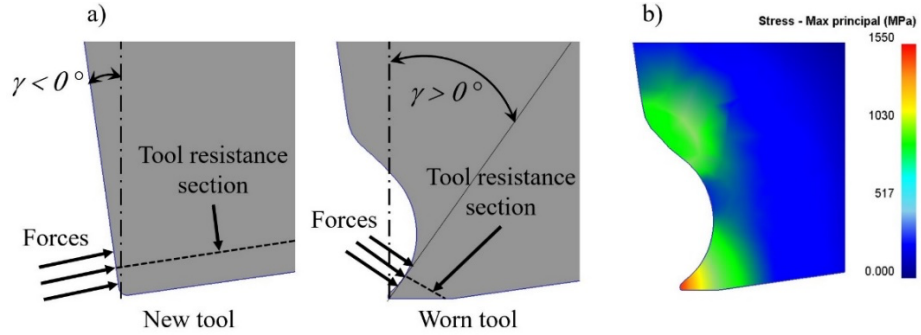

Figure 10. a) Effect of wear on effective rake angle, b) Tensile stresses on a worn tool.

3.2. Experimental results

The implemented wear model has been validated by the comparison of the simulated tool wear with the experimental one. The evolution of experimental and simulated crater wear (*KT*) and flank wear (*VB*) during the cutting time for all the tests is depicted in the plots of figure 11. The good match amongst the different results is clearly visible. Therefore, the employment of the combined rake-flank tool wear model allows to correctly simulate the wear behavior as a function of the cutting parameters, avoiding the need of performing costly and time-consuming experimental tests and permitting an optimization of process parameters. Moreover, the implementation of this new tool wear model grants the prediction of the effective rake angle, due to the growing of crater wear. Figure 12 shows the evolution of simulated effective rake angle during time, normalized respect the tool life of each test. The increase of the crater wear changes the effective rake angle from a negative to a positive value.

It is important to supervise the value of this angle since PCBN tools present extremely high resistance to compressive stresses but poor to tensile ones. Consequently, the application of a negative rake angle is recommended to enhance compressive stresses on them. Conversely, when the rake angle is positive tensile stresses increases. Figure 12 underlines the independency of rake angle limit leading to tool breakage from process parameters, in fact its value ranges between 25° to 30° for all the tests.

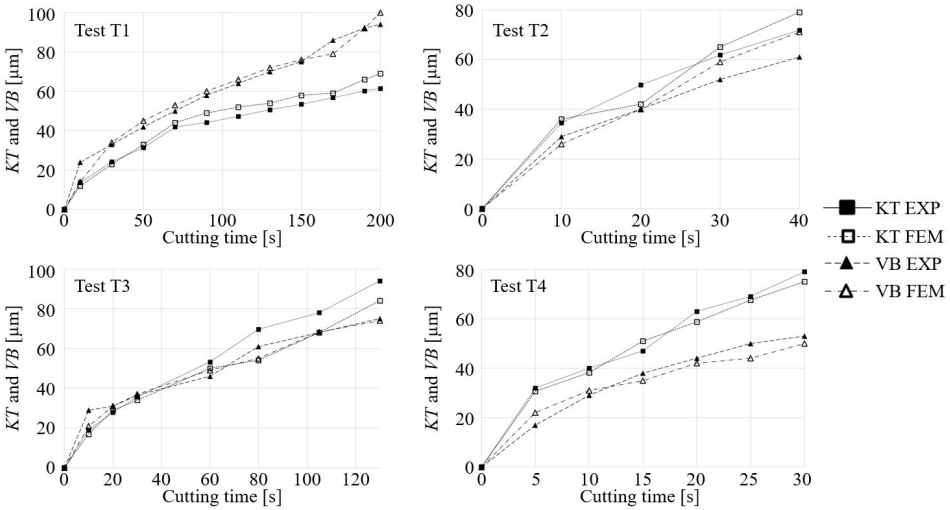

Figure 11. Comparison between experimental and simulated *KT* and *VB* values.

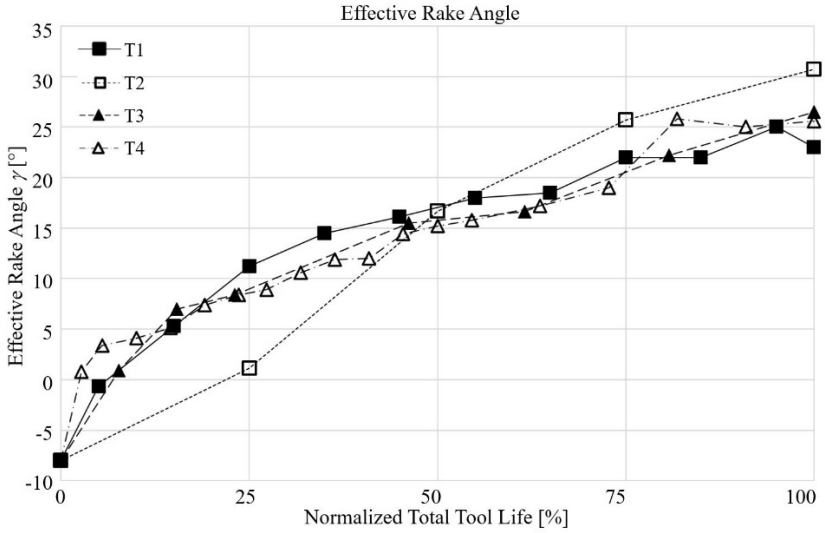

Figure 12. Evolution of effective rake angle as a function of the normalized tool life.

4. Conclusions

In the present paper the results achieved from a study on tool wear simulation of PCBN inserts when cutting AISI 52100 hardened steel, aimed to improve the quality and the reliability of FEM analysis of machining operations, has been presented. Simulations replicating experimental tests has been performed. Moreover, a coupled abrasive-diffusive wear model able to update the geometry of the worn tool during machining simulations, have been implemented into a FEM engine by means of a suitable subroutine. Experimental and simulated wear parameters have been compared in terms of crater depth and flank wear width. This comparison demonstrated the capability of the FEM model to closely reproduce the tool wear throughout the cutting time. The validated FEM model has been also employed to analyze the effect of tool wear on the effective rake angle of the worn insert. This underlined how the increase of crater depth leads to a modification of the rake angle from a negative to a positive value, reducing the tool resistance section. The combination of this with the high brittleness of PCBN material, has been individuated as the mechanism of failure of the tool, bringing to premature breakage. Hence, the proposed FEM strategy can be applied to optimize the process

parameters by continuously monitoring crater and flank wear evolution, preventing catastrophic rupture, and allowing a correct replacement of the tool.

References

[1] G. Bartarya, S.K. Choudhury, "State of the art in hard turning", *International Journal of Machine Tools & Manufacture*, vol. 53, pp. -14, 2012.
[2] W.F. Sales, J. Schoop, L.R.R. da Silva, A.R. Machado, I.S. Jawahir, "A review of surface integrity in machining of hardened steels", *Journal of Manufacturing Processes*, vol. 58, pp. 136-162, 2020.
[3] C. Cappellini, A. Attanasio, G. Rotella, D. Umbrello, "Formation of white and dark layers in hard cutting: Influence of tool wear", *International Journal of Material forming*, vol. 3, pp. 455-458, 2010.
[4] A.V. Pradeep, D.L. Raju, S. Ramakrishna, "Cutting force analysis in hard turning of AISI 52100 steel using multi-layer coated carbide inserts – RSM approach", *Materials today: Proceedings*, https://doi.org/10.1016/j.matpr.2019.07.369
[5] G. Poulachon, A. Moisan, I.S. Jawahir, "Tool-wear mechanisms in hard turning with polycrystalline cubic boron nitride tools", *Wear*, vol. 250, pp. 576-586, 2001.
[6] Y. Huang, Y.K. Chou, S.Y. Liang, "CBN tool wear in hard turning: a survey on research progresses", *The International Journal of Advanced Manufacturing Technology*, vol. 35, pp. 443-453, 2007.
[7] M.A. Yallese, K. Chaoui, N. Zeghib, L. Boulanova, J-F. Rigal, "Hard machining of hardened bearing steel using cubic boron nitride tool", *Journal of Materials Processing Technology*, vol. 209, pp. 1092-1104, 2009.
[8] A. Attanasio, D. Umbrello, C. Cappellini, G. Rotella, R. M'Saoubi, "Tool wear effects on white and dark layer formation in hard turning of AISI 52100 steel", *Wear*, vol. 286-287, pp. 98-107, 2012.
[9] F. Zemzemi, H. Khochtali, W.B. Salem, B. Alzahrani, M-L. Bouazizi, "Analytical multi-physics model of microstructure changes in hard turning of AISI 52100 steel: prediction of thicknesses of white and dark layers", *The International Journal of Advanced Manufacturing Technology*, vol. 112, pp. 2755-2771, 2021.
[10] Y. Huang, T.G. Dawson, "Tool creater wear depth modeling in CBN hard turning", *Wear*, vol. 258, pp. 1455-1461, 2005.
[11] S. Gordon, P. Phelan, C. Lahiff, "The effect of high speed machining on the crater wear behaviour of PCBN tools in hard turning", *Procedia Manufacturing*, vol. 38, pp. 1833-1848, 2019.
[12] S. Chinchanikar, S.K. Choudhury, "Predictive modeling for flank wear progression of coated carbide tool in turning hardened steel under practical machining conditions", *The International Journal of Advanced Manufacturing Technology*, vol. 76, pp. 1185-1201, 2015.
[13] D. Singh, P.V. Rao, "Flank wear prediction of ceramic tools in hard turning", *The International Journal of Advanced Manufacturing Technology*, vol. 50, pp. 479-493, 2010.
[14] U.M.R. Paturi, S. Cheruku, V.P.K. Pasunuri, S. Salike, "Modeling of tool wear in machining of AISI 52100 steel using artificial neural networks", *Materials Today: Proceedings*, https://doi.org/10.1016/j.matpr.2020.06.581
[15] A. Attanasio, E. Ceretti, A. Fiorentino, C. Cappellini, C. Giardini, "Investigation and FEM-based simulation of tool wear in turning operations with uncoated carbide tools", *Wear*, vol. 269, pp. 344-350, 2010.
[16] D. Umbrello, J. Hua, R. Shivpuri, "Hardness based flow stress for numerical modeling of hard machining AISI 52100 bearing steel", *Mater. Sci. Eng.–A*, vol. 347, pp. 90-100, 2004.
[17] N.I.N. Zorev, "Metal Cutting Mechanics", Pergamon Press, Oxford, New York, xv, pp. 526, 1966.